Earthquake Geotechnical Engineering for Protection and Development of Environment and Constructions – Silvestri & Moraci (Eds)
© 2019 Associazione Geotecnica Italiana, Rome, Italy, ISBN 978-0-367-14328-2

Liquefaction risk assessment: Lesson learned from a case study

G. Modoni, R.L. Spacagna, L. Paolella, E. Salvatore & A. Rasulo
University of Cassino and Southern Lazio, Cassino, Italy

L. Martelli
Regione Emilia-Romagna, Direzione Generale Cura del Territorio e dell'Ambiente, Servizio geologico, sismico e dei suoli, Italy

ABSTRACT: A detailed and comprehensive assessment of risk is the basis to protect communities and assist decision-making towards the sustainable management of territories. For liquefaction this process implies to simultaneously investigate seismic hazard, susceptibility of the subsoil, vulnerability of structures, economic and social relevance of critical infrastructures and ultimately build a comprehensive multi-level model that considers the interaction among all aspects. Developing a methodology to achieve this goal is the scope of Liquefact, a EU H2020 project. A case study pervasively affected by liquefaction damages is here studied as a real scale scenario to identify the main factors of uncertainty. The available data concerning seismic motion, subsoil and building characteristics, damage and economic loss are used to develop a methodology aimed at quantifying and reducing uncertainties in the spatial distribution of risk.

1 INTRODUCTION

Although liquefaction is not as dramatic and shocking as other earthquake effects like collapse of structures, landslides and tsunamis, it is similarly harmful for the communities in terms of economic and social effects. The fact that liquefaction is a secondary hazard in the context of earthquake-induced losses by no means diminishes its importance, as the extensive physical damage produced on buildings and lifelines is just a part of the impact and injuries being aggravated by the prolonged reduced serviceability of the critical infrastructures (Macaulay et al. 2009). The experience of real events has shown that damage usually occurs not only on the building asset, but also the facilities connected directly or indirectly to the productive systems (roads, waterways, electric and communication lines), in this way undermining for long time the whole social organization and the recovery capacity of the communities.

The above concerns raise the need for involving stakeholders, boards, governmental agencies, regulators, suppliers of services, investors in an unified process aimed at increasing safety, preparedness and survivability. Awareness of risks, vulnerability and of the capability to deal with them enables communities to make informed, tactical and strategic decisions. A comprehensive assessment of risks that correctly estimate the distribution over the territory of hazard, vulnerability and exposure becomes fundamental to undertake appropriate mitigation actions and optimize the budget allocation.

The holistic assessment of liquefaction risk at different scales, from single structures to aggregates, and the improvement of community resilience is the goal of Liquefact, a project funded by the European Union Horizon 2020, Research and Innovation Programme (#700748, 2016). Thanks to the spread of geoinformatics, rich spatial databases can be nowadays created, empirical connections, mechanical based schemes or artificial intelligence tools can be adopted to connect information and map the results of complex analyses. Liquefaction risk assessment takes noticeable advantage from the assembly into the same geographically

information system of data on seismic hazard, geotechnical properties of the subsoil, structural and functional characteristics of buildings and infrastructures.

There is ample recognition within the experts that case histories, where the above information can be conjugated with response observed on site and post-earthquake surveys of damage can serve to develop, calibrate or validate liquefaction analyses free from the subjective judgment. The present paper illustrates how the above scope is pursued on a small urban aggregate pointing out on the difficulties, drawbacks and uncertainties related with the assessment.

2 LIQUEFACTION RISK ASSESSMENT

In current practice, liquefaction susceptibility, triggering, and consequences are deterministically evaluated without explicitly considering the uncertainty related to the various components of the analysis or the performance metric. However, considering this issue is central as the knowledge of nearly all factors, ground motion, subsoil and building properties is affected by aleatory and epistemic uncertainties. Performance-based earthquake engineering offers a rational and consistent way to consider uncertainty through probabilistic evaluations. For a generic system with its lifecycle, a risk of any nature can be computed writing the following convolution integral that convolutes the probability of demand p(D) (Hazard) and the consequent losses connected to the demand P(L|D) (Vulnerability):

$$P(L) = \int_{D} P(L \backslash D) * p(D) \tag{1}$$

A correct application of eq.1 should separately disclose and quantify the uncertainties on:

- the potentially critical scenarios
- the models describing the response of the system
- the quantification of relevant parameters
- the risk evaluation

For seismic risk, eq.1 can be expressed applying the performance-based earthquake assessment (PEBA) cascade methodology defined by the Pacific Earthquake Engineering Research (PEER) Center (Cornell & Krawinkler 2000) and depicted in Fig.1.

Eq.1 is transformed as follows where the function p(D) is exploded considering the different factors defining the cascade phenomenon:

$$P(L) = \int_{IM} \int_{EDP} \int_{DM} P(VD|DM) * p(DM|EDP) * p(EDP|IM) * p(IM) \tag{2}$$

p(IM) is the probability that a seismic event of intensity measure IM occurs during the lifecycles of the system, p(EDP|IM) is the density probability of the engineering demand parameter (EDP) for the given IM, p(DM|EDP) is the probability that a physical damage occurs on the structural component of the system for a given EDP and P(VD|DM) is an cumulative

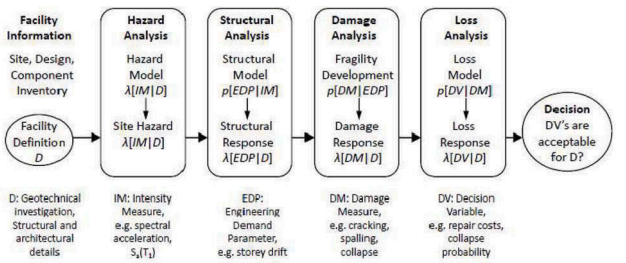

Figure 1. Probabilistic definition of risk assessment (Cornell & Krawinkler 2000).

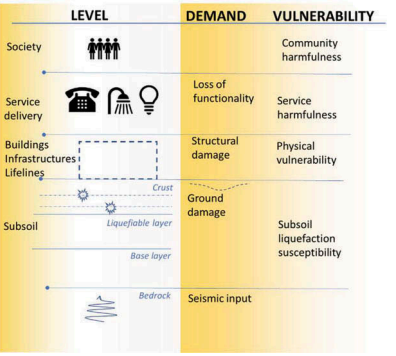

Figure 2. Definition of risk assessment for seismic liquefaction.

probability of the assumed evaluator of the system performance for a given damage DM (Lee and Mosalam 2006; Moehle 2003; Porter 2003; Comerio 2005; Krawinkler 2005; Mitrani-Reiser et al. 2006).

'Considering the sequence of subsystems involved in seismic liquefaction (see Fig.2), the PEBA methodology can be expressed quantifying the uncertainties on earthquake intensity, ground motion, structural response, physical damage, and economic or human losses. The scheme of Fig.2 shows that the above formula can be applied to the whole system or to subsystems composed of one or more elements, provided demand and vulnerability are properly defined. Changing the position of the lines bordering the vulnerable system (on the right column of the figure), different definitions of hazard and risk are obtained.

In particular, the earthquake can be considered as the primary hazard factor and liquefaction occurs if the soil has specific characteristics, namely a grain size distribution composed of sand with limited fine content, sufficiently low density and saturation. Therefore, the combination of earthquake and subsoil response determines the demand for the structure positioned at the ground level. However, physical damage for the latter can be computed considering the subsoil-structures as a unique coupled system or evaluating the response of the two components separately. In the first case the earthquake intensity measure IM becomes also the engineering demand parameter EDP and the vulnerability function p(DM|EDP) quantifies the response of the subsoil-structure system for the given seismic input. In the second case, the soil response provides the demand function p(EDP|IM) for the structure and physical vulnerability is computed considering the p(DM|EDP) function for the sole structure. HAZUS code (FEMA 1998) adopts this second approach considering soil liquefaction in a group of secondary hazards called ground failures affecting building assets and infrastructure networks.

Following the sequence depicted by Fig.2, physical damage represents the demand for the delivery capability of the system whose vulnerability is defined by a function that relates the loss of serviceability to the different levels of damage. Finally, the latest level of risk assessment concerns the community: it is harmed by the loss of safety and serviceability and risk can be assessed in terms of deaths, injuries, loss of incomes, damage to cultural and environmental heritage.

The terms of eq.2 can be quantified in different manners, sometimes with probabilistic inference of statistical observations, sometimes applying theoretical models with stochastically variable inputs, sometimes with less objective procedures. For instance, it is customary to express severity of damage in terms of financial losses based on expert judgement, qualitative estimates or even rules of thumb that make the process unavoidably subjective.

Some of the relations of eq.2 (e.g. p(A|B) with A and B indicating generic variables) can be established on a deterministic basis (A=f(B)). In this case p(A|B) can be expressed with a Dirac function, i.e. equal to ∞ for A=f(B) or 0 for A≠f(B). The above issues are addressed in the next paragraphs looking at the different factors concurring to determine liquefaction.

3 SEISMIC INPUT

As for any other seismic assessment, the characteristic seismic input at the rigid base can be retrieved on hazard zonation maps (e.g. www.share-eu.org) that generally provide seismic spectra for different return periods T_r. Therefore, given a lifecycle of the considered structure, the probability associated to each event can be computed as function of T_r. Possible amplifications must then be considered for the specific site, referring to the subsoil types defined in the standards (e.g. Fardis et al., 2005) and considering maps giving information on the subsoil (e.g. https://earthquake.usgs.gov/data/vs30/) or, preferably, adopting seismic microzonation studies. Alternatively, a seismic response analysis can be performed on the site to be studied. Lately, the scenario earthquakes can be obtained in terms of response spectra, artificial, recorded or simulated accelerograms quantifying IM for each of them. The choice essentially depends on the quality of available data for subsoil characterization, connected with the extent of the studied area.

One main question arises on the Intensity Measure relevant for liquefaction. Studying the performance of different IMs on liquefaction versus advanced numerical calculations, Karimi and Dashti (2017) observed that the evolutionary settlements of structures depend on intensity, duration and frequency content of the ground motion and concluded that cumulative energy is a more appropriate to represent intensity measure, more than peak variables. They propose the cumulative absolute velocity (Campbell & Bozorgnia, 2011) as a potential candidate as also recently assumed by Bray & Macedo (2017) and Karamitros et al., (2013). Other authors (e.g. Youd et al., 2002; Youd & Perkins, Bardet et al., 2002; Rauch & Martin, 2000) combine magnitude, distance from the rupture and peak ground acceleration. Tokimatsu & Seed (1987) adopt the cyclic stress ratio CSR introduced by Seed & Idriss (1971) corrected (e.g. Idriss & Boulanger, 2010) for magnitude values.

4 SUBSOIL RESPONSE

The quantification of subsoil response moves along three subsequent steps (e.g. Bird et al., 2006): determine susceptibility to liquefaction based on qualitative criteria; evaluate the conditions for liquefaction triggering by the scenario earthquake; predict the expected demand for the structure (ground deformations or other proxies of damage).

The first step is normally accomplished at the geological level, involving larger portions of the territory and considering broad subsoil classifications like the one proposed by Youd & Perkins (1978). This criterion emphasizes the depositional environment and age of the deposit observing that liquefaction susceptibility is rather high for Holocene or more recent (e.g. artificial) deposits, low or very low for Pleistocene or older ones. A remarkable example is the strong correlation noticed in Figure 3 between the distributions of paleo-rivers and liquefaction manifestation during the 2012 seismic sequence in Emilia Romagna. The overlapping is particularly evident between the municipalities of Sant'Agostino and Mirabello. Historical documents report that the Reno river was crossing this zone for a period of three hundred years, from the half of fifteenth to the half of eighteen century, releasing sediments with very high rates (10÷30cm/year).

Once the above conditions are ascertained, the co-existence of paramount factors, i.e. grain size distribution and water level must be determined at a smaller scale with a more refined investigation. To estimate triggering, many standards worldwide (e.g. NZGS, 2016; Yasuda e Ishihawa, 2018; DPC, 2017) adopt relations between in situ soil density and cyclic shear stress induced by ground shaking. For a given soil profile, the triggering of liquefaction at different depths is evaluated computing a safety factor (FSL) given by the ratio of the cyclic stress ratio τ/σ'_v producing liquefaction (CRR) and the one induced by the earthquake (CSR). Robertson & Wride (1998), Idriss & Boulanger (2010) and Boulanger & Idriss (2015), provide empirical formulations of the Cyclic Resistance Ratio based on the survey of liquefaction and the results of common geotechnical in-situ tests (CPT, SPT, Vs profile).

The above relationships are derived deterministically as medians of case history databases. As such, they are affected by uncertainties arising from the definition of CSR (model uncertainty on the triggering relationship) and from the quality and interpretation of investigation

Type of deposit (1)	General distribution of cohesionless sediments in deposits (2)	Likelihood that Cohesionless Sediments, When Saturated, Would Be Susceptible to Liquefaction (by Age of Deposit) <500 yr (3)	Holocene (4)	Pleistocene (5)	Pre-pleistocene (6)
(a) Continental Deposits					
River channel	Locally variable	Very high	High	Low	Very low
Flood plain	Locally variable	High	Moderate	Low	Very low
Alluvial fan and plain	Widespread	Moderate	Low	Low	Very low
Marine terraces and plains	Widespread	—	Low	Very low	Very low
Delta and fan-delta	Widespread	High	Moderate	Low	Very low
Lacustrine and playa	Variable	High	Moderate	Low	Very low
Colluvium	Variable	High	Moderate	Low	Very low
Talus	Widespread	Low	Low	Very low	Very low
Dunes	Widespread	High	Moderate	Low	Very low
Loess	Variable	High	High	High	Unknown
Glacial till	Variable	Low	Low	Very low	Very low
Tuff	Rare	Low	Low	Very low	Very low
Tephra	Widespread	High	High	?	?
Residual soils	Rare	Low	Low	Very low	Very low
Sebka	Locally variable	High	Moderate	Low	Very low
(b) Coastal Zone					
Delta	Widespread	Very high	High	Low	Very low
Esturine	Locally variable	High	Moderate	Low	Very low
Beach					
High wave energy	Widespread	Moderate	Low	Very low	Very low
Low wave energy	Widespread	High	Moderate	Low	Very low
Lagoonal	Locally variable	High	Moderate	Low	Very low
Fore shore	Locally variable	High	Moderate	Low	Very low
(c) Artificial					
Uncompacted fill	Variable	Very high	—	—	—
Compacted fill	Variable	Low	—	—	—

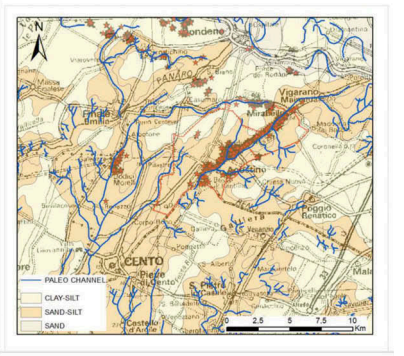

Figure 3. Geological susceptibility criterion (Youd & Perkins 1978) and distribution of liquefaction damage caused by the 2012 earthquakes in Emilia Romagna (Italy).

(measurement or parameter uncertainty) (Toprak et al. 1999; Cetin et al. 2004). Analyzing a database of 230 cases,

Idriss & Boulanger (2010) derive the following relation to estimate the conditional probability of liquefaction for known values of CSRM=7.5,σ‘=1atm and the standard penetration resistance corrected for the presence of finer soil N1,60,cs:

$$P_L((N_1)_{60cs}, CSR_M = 7.5, \sigma'_V = 1atm) = \Phi\left[\frac{-\frac{(N_1)_{60cs}}{14.1} + \left(\frac{(N_1)_{60cs}}{126}\right)^2 - \left(\frac{(N_1)_{60cs}}{23.6}\right)^3 + \left(\frac{(N_1)_{60cs}}{25.4}\right)^4 - 2.67 - ln(CSR_M = 7.5, \sigma'_V = 1atm)}{\sigma_{ln(R)}}\right] \quad (3)$$

The authors find that a standard deviation $\sigma_{ln(R)}$ equal to 0.13 correctly represents variability.

Even considering with probabilistic models the uncertainty associated with the ground-motion estimation and the likelihood of liquefaction triggering, the above procedures are affected by other uncertainties related with measurement biases of in situ data (Baecher & Christian 2003). In spite of a tendency to discipline the execution and interpretation of subsoil investigation for improving consistency, quality and reliability (e.g. NZGS, 2016), the major part of data presently available for risk assessment have been obtained in previous times with out of date standards. An attempt to fill this gap is proposed by Madiai et al. (2016) who performed an experimental study to convert the results of mechanical CPT into equivalent electrical CPT data.

Inconsistency of investigation is one of the major causes of error in interpolating information over the areas. Tests performed at mutual distance of few meters may give markedly different estimates of important parameters. Geostatistical tests (Chilès & Delfiner. 2012) are very helpful to identify singularities, e.g. where experimental results differ too much from the spatial trend inferred from contiguous investigations, and to quantify uncertainty of the estimate in each position. From the viewpoint of the probabilistic risk assessment, this result quantifies the reliability of the estimate and the uncertainty associated with the subsoil characterization and provides a criterion to plan optimal campaigns to integrate information.

As an example, Figure 4 shows the map of liquefiable layer thickness over San Carlo Emilia (Italy), a village struck by severe liquefaction during the 2012 earthquake (see Fig.3). The left

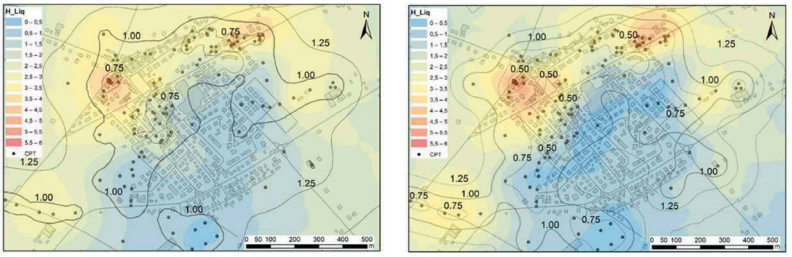

Figure 4. Liquefiable layer thickness over San Carlo Emilia drawn from all CPT tests (a) and after removing inconsistent data (b). (Contour lines represent the standard deviation of error).

figure reports the map built with all available CPT tests, the right one shows the same map obtained after removing some inconsistent tests (CPT positions are marked with dots). The estimate of liquefiable layer is affected by the water table position, that was here taken from a study of (RER, 2012).

The exam to evaluate consistency/inconsistency is based on the difference between variables estimated directly from the test and from interpolation of contiguous data. CPT logs for which this difference exceed 5% and 95% fractile of the error distribution were removed. This operation slightly modifies the map, but the contour lines that quantify the estimate error show an improved quality of the information. The remaining error is mainly connected with the density of information (in the present case, CPTs were mostly performed close to damaged buildings), and thus a criterion is obtained to select areas where investigation is more needed.

The effects at ground level are normally predicted (e.g. NZGS 2016; DPC 2017) with indicators of severity that empirically synthesize the paramount factors dictating liquefaction in free field conditions. They are computed as integral over fixed depths of a function of the safety factor *f*(FSL) weighted with a function of depth from the ground level w(z).

$$INDEX = \int_{zmax} f(FSL) * w(z) dz \tag{4}$$

Table 1 shows a list of the most common indexes. In spite of simplicity that makes these indicators appealing for an extensive assessment, they suffer the implicit limitation of quantifying the subsoil response with a sum of contributions from all susceptible layers (FSL<1) located at different depths, ignoring in this way any possible mechanical and hydraulic cross-interaction between susceptible layers located at different depths (Cubrinovski 2017).

The question can be seen from Figure 5 that shows a coupled hydro-mechanical analysis carried with the Finite Difference Code FLAC 2D (Itasca 2016) simulating the response of sand with a non-linear model (PM4Sand by Boulanger & Ziotopoulou 2012) that accounts for the strain accumulation due to repetitive loading. The simulation inspired by a stratigraphy of San Carlo reveals that the onset of liquefaction in the lower sandy layer ($r_u=\Delta u/\sigma'_{vo}\approx 1$) prevents the further increase of pore pressure in the upper layers.

This phenomenon affects the reliability of assessment with simplified methods in the case of multilayered systems and thus a preliminary check is necessary to verify if the schematization with three layers (base, liquefiable layer and crust) is applicable to the studied case and if more sophisticated models must be adopted. Millen (2019) propose a test based on CRR to verify the equivalence of soil profiles derived from CPTU tests with three layers models described by the combination of depth (H_{crust}), thickness (H_{liq}) and mean CRR of the liquefiable layer. This test gives positive results for all CPT performed in San Carlo Emilia, basically because the liquefiable layer in this case is induced by a continuous depositional event occurred over a limited time period. Figure 6 shows a view of the three-dimensional model of San Carlo adopted for the present analysis.

Table 1. Severity liquefaction indicators proposed in the literature.

INDEX	REFERENCE	f (FSL)	w(z)	Z
LPI	Iwasaki, 1978	$1 - \mathrm{FSL} \quad \text{if FSL} < 1$ $0 \quad \text{if FSL} \geq 1$	$10 - 0.5z$	$Z_{min} = 0 Z_{max} = 20m$
LPIish	Maurer, 2014	$\{1 - FSL \;\; if \;\; FSL \leq 1 \cap H1 \cdot m(FSL) \leq 3$ $0 \;\; otherwise$ $m(FSL) = \exp\left(\frac{5}{25.56(1-FSL)}\right) - 1$	$\frac{25.56}{z}$	$Z_{min} = H1 Z_{max} = 20m$
W	Zhang et al., 2002	$\varepsilon_v = \varepsilon_v \; (FSL, qc1N_{cs} \;)$	-	$Z_{min} = 0 Z_{max} = \max depth$
LDI	Zhang et al., 2004	$\gamma_{max} = \gamma_{max} \; (FSL, \;\; qc1N)$	-	$Z_{min} = 0 Z_{max} < 23m$
LSN	van Ballegooy, 2014	$\varepsilon_v = \varepsilon_v \; (FSL, qc1N_{cs} \;)$	$\frac{1000}{z}$	$Z_{min} = 0 Z_{max} = 20m$

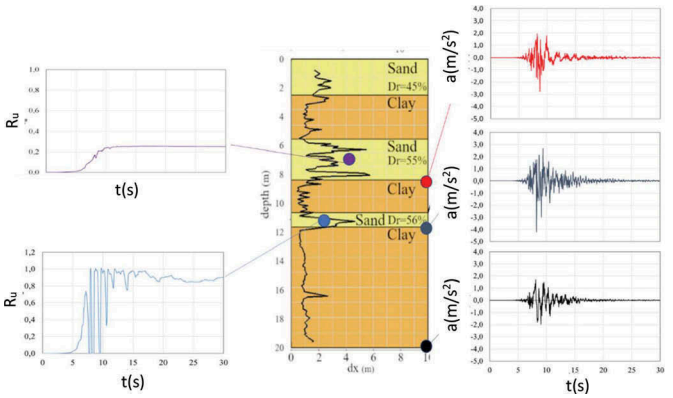

Figure 5. Numerical analysis of seismic wave propagation through a multi-layered subsoil.

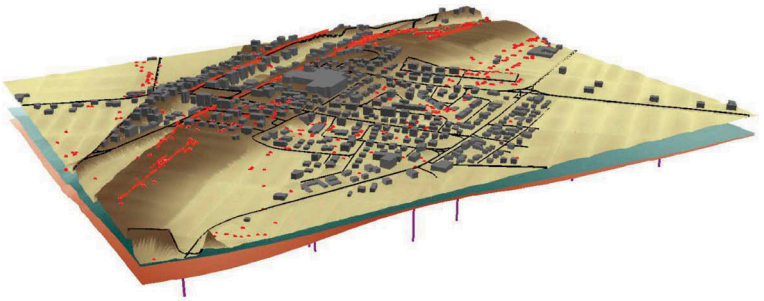

Figure 6. Three-dimensional subsoil model of San Carlo Emilia (green and brown surfaces represent respectively top and bottom surfaces of the liquefiable layer – the vertical scale is five times larger than horizontal one).

5 STRUCTURAL DAMAGE

For a given hazard, the physical damage induced by liquefaction on structures and infrastructures depends on their typology, planimetric extension and capability to adsorb absolute and

differential movements. The estimate of losses is by far more complex than the assessment of liquefaction occurrence in the subsoil (Bird et al., 2006). Uncertainties basically stem from the following reasons:

- Coupling of liquefaction and ground shaking
- Identify damage mechanisms and define a demand for liquefaction
- Classify damage into levels
- Categorize structure response into homogenous groups

The above concerns become even more relevant and problematic for buildings due to the larger variety of structural typologies and construction materials adopted worldwide.

The issue of combined ground shaking and liquefaction has been largely debated. More often buildings that have undergone liquefaction do not exhibit ground shaking damage, giving the idea that a base isolation could be induced by the liquefied soil on the building. However, evidences of buildings damaged by both shaking and liquefaction suggest that severe ground shaking might take place before the groundwater pressure builds up. Bird et al. (2005) claim that the differential settlement induced by liquefaction on framed buildings causes a drift of columns additional to that produced by shaking and thus structures previously affected by shaking are more vulnerable to liquefaction. Following this idea, these authors propose a cumulative analytical methodology considering permanent shaking deformation as a reduction of the building capacity against liquefaction. The connection between the two mechanisms is even more evident for masonry structures.

Focusing solely on the effects of liquefaction, a list of possible building damages is provided by van Ballegooy (2014) together with the threshold movements defining the level of damage. Differential settlements or horizontal movements dictated by inhomogeneous load distributions and stratigraphic conditions (e.g. inherent variability of homogeneous subsoil and, moreover, boundary between liquefied and non-liquefied soils) are recognised among the most critical causes of damage. Rigid body movements like uniform settlement, tilting and horizontal sliding may add, increasingly affecting aesthetic, serviceability and, ultimately, stability of buildings. The relative weight among mechanisms is mainly dictated by the stiffness of the structural system with a paramount role of its foundation, whether made of isolated footings, continuous beams or pads, pile reinforcement. A classification of severity levels cumulatively including shaking and liquefaction has been proposed by Bird et al. (2006). They define four classes of damage, namely slight, moderate, extensive and complete based on repairability of the building. However, as pointed out by the same authors, a general applicability of this criterion is affected by the strong dependency of the fixed limits on the type of structure, on the suitability of buildings and foundation to sustain repair works, plus several other factors dictated by the local practice. van Ballegooy et al. (2014) (Figure 7) distinguishes damage according to the deformation mechanisms activated on the building and on the extent of settlement. A more general classification of damage on buildings of different typology, not just referred to liquefaction, is provided by Poulos et al. (2001) where a distinction is made among the type of structure (framed, masonry, bridges) and level of damage. In all cases, predicting the overall kinematics of buildings is not easy, moreover for large-scale assessment where geotechnical and structural information are largely incomplete. Following a methodology adopted for the serviceability limit state analysis of foundations under static loads (Grant et al. 1974), differential settlements quantified by the relative rotation β have been related to the absolute settlements of the building.

Once the equivalence between absolute settlement and distortion is established, it is readily seen that the classification criteria defined by van Ballegooy (Figure 7) and Poulos (Figure 8.a) lead to similar limit values of settlements. In both cases, damage is triggered for absolute settlements in the range 10–50 mm, being severity dependent on the building type. Absolute settlements could thus be considered as possible Engineering Demand Parameters to estimate damage.

This procedure is experimentally checked against the 2012 earthquake in San Carlo Emilia, exploiting the available information on subsoil and building characteristics and on the surveyed damage (e.g. Fioravante et al. 2013). Settlements have been computed with a formula proposed by Karamitros et al. (2013). The formula considers the principal factors dictating the mechanical response of the foundation: the seismic input is expressed via a cumulated

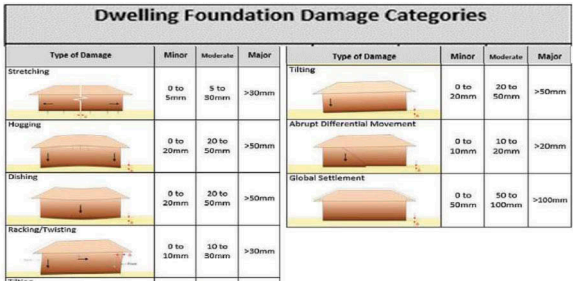

Figure 7. Type and level of damage caused on buildings by liquefaction (van Ballegooy, 2014).

Type of structure	*Type of damage/ concern*	*Quantity to be considered*	*Limiting value*
Framed building and reinforced load bearing walls	Structural damage	Angular distortion	1/150–1/250
	Cracking in walls and partitions	Angular distortion	1/500 (1/100–1/1400 for end bays)
	Visual appearance	Tilt	1/300
	Connection to services	Total settlement	50–75 mm (sand) 75–135 mm (clay)
Tall buildings	Operation of lifts and elevators	Tilt after lift installation	1/1200–1/2000
Structures with unreinforced load bearing walls	Cracking by sagging	Deflection ratio	1/2500 (L/H = 1) 1/1250 (L/H = 5)
	Cracking by hogging	Deflection ratio	1/5000 (L/H = 1) 1/2500 (L/H = 5)
Bridges – general	Ride quality	Total settlement	100 mm
	Structural distress	Total settlement	63 mm
	Function	Horizontal movement	38 mm
Bridges – multiple span	Structural damage	Angular distortion	1/250
Bridges – single span	Structural damage	Angular distortion	1/200

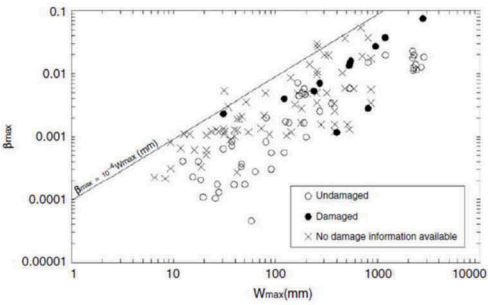

Figure 8. Classification of damage (a. from Poulos et al., 2001), empirical relation between maximum absolute settlement and angular distortion (b) for shallow and piled foundations (Viggiani et al., 2013).

energy variable; settlement is proportional to the ratio between applied and limit unit vertical load. The latter, computed with the classical trinomial formula and as such accounts for excess pore pressure development, friction ratio of the liquefiable sand, thickness and shear strength of the crust, size and shape of the foundation and load discharged onto the soil.

The initial friction angle of the sand and shear strength of the crust have been fixed equal to respectively 30° and 30 kPa, matching the prediction with the formula with the results of numerical simulations performed with a Finite Difference code (the same adopted in Figure 5). To this aim, a strip foundation having size equal to 10 m carrying a unit load of 50 kPa has been considered on a three layers models (see Figure 9a) calibrating the soil constitutive models on laboratory and site experiments (Fioravante et al., 2013) and varying parametrically the thicknesses of the crust (from 2 to 12 m), the thickness of the liquefiable layers (from 2 to 8 m) and the seismic input. The agreement between the two predictions (Figure 9b), proves to be very good for low settlements, worse for larger settlements basically corresponding to low crust thicknesses.

The formula has been then extensively applied to compute settlements caused on each building of San Carlo by the May 20th 2012 earthquake (6.1 M_w).

To this aim a database has been created reporting for each building the footprint dimensions, the number of storeys, thicknesses of crust and liquefiable layers. Relevant issues for calculation are applied load, foundation type and dimensions. To this aim it is considered that the building typology is rather homogeneous, being structures mostly made of brick walls with strip foundations. Considering the local practice, an average width of 0.8 m has been assigned to the foundations, assuming that they cover half of the footprint area. The applied unit load is then computed subdividing uniformly spreading on this area the total load, proportional to the number of floor and extension of the building. Predicting the damage of each building is out of the scope of the present work as many relevant information, primarily the structural characteristics of the buildings and the mechanical properties of the foundation soil, are unknown and assumed as constant. However, the map of Figure 10 shows that the analysis captures rather closely the liquefaction evidences, sand ejecta and ground fissures, noticed at the ground level soon after the earthquakes Fioravante et al.2013) and the spatial distribution of damaged buildings.

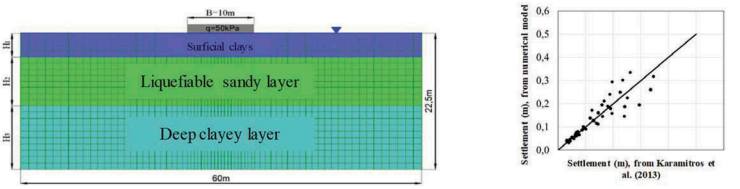

Figure 9. Calibration of Karamitros (2013) formula for the case of San Carlo Emilia.

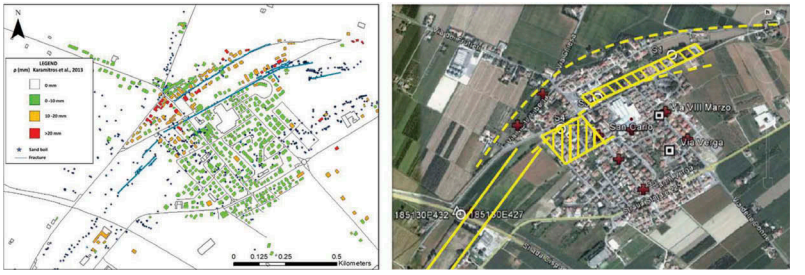

Figure 10. Settlements of buildings computed with Karamitros et al. (2013) formula (a) and damage (b) after the 2012 May 20th (M_w 6.1) earthquake in San Carlo (Fioravante et al. 2013).

The effectiveness of absolute settlements as engineering demand parameter has then been evaluated on a statistical basis, considering the distribution of damaged buildings recorded by the Emilia Romagna Region. To this end, a catalogue has been created examining the reports of the investigation carried out immediately after the earthquake and all technical reports produced for reconstruction purposes. Out of a total of 663 buildings, about 88 suffered structural damage caused by earthquake. A deeper check has then been made to distinguish on each building the effects of shaking and liquefactions and to consider only the latter for the present analysis. The curves expressing the cumulated probability of damage versus the computed absolute settlement ρ for the different classes of buildings have been then reconstructed with the Bayes theorem:

$$P(Damage|\rho) = \frac{P(\rho|Damage) * P(Damage)}{P(\rho)} \tag{5}$$

The curve reported for all buildings shows a correlation between the two variables proving that absolute settlement can be assumed as a proxy of damage. The relation becomes even more evident if a distinction is made based on the age of construction. To this aim, the structures built before 1954 have been isolated, extracting them from an aerial photograph taken in that year, and the same probability curves have been computed. This subcategory reveals a higher percentage of damaged buildings (73 over a total number of 268) possibly due to a lower quality of the manufacture. According to the report of local engineers, the foundations of buildings made before world war II basically consisted in a prolongation to a limited depth of the upper masonry. With time, the new buildings were founded on strips made of reinforced concrete or at least some reinforcement was added at the base of the strip foundation made with bricks. For the sake of risk assessment, a more detailed survey of the structural and foundation characteristics of buildings would certainly improve accuracy.

6 CONCLUSIONS

In the present study the uncertainties affecting liquefaction risk assessment are examined on a case study to understand criticalities and provide a methodology for future guidelines. Quantifying reliability of the assessment is fundamental to understand how the lack of knowledge

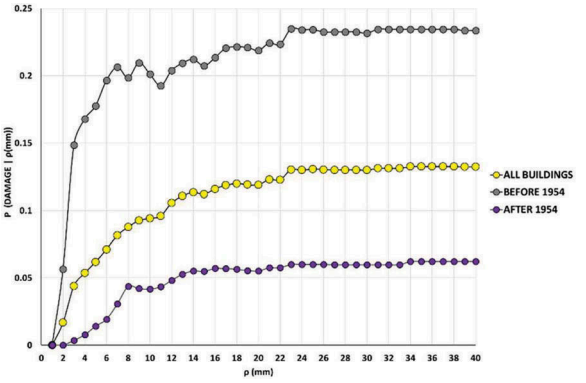

Figure 11. Cumulated probability of damage versus the absolute settlement ρ for the case study of San Carlo Emilia.

affects results, to avoid misuses of the outcomes or wrong conclusions. While realistic analyses are possible at the scale of single building, reproducing with numerical codes structural characteristics, subsoil stratigraphy and geotechnical properties, accuracy drops when faster procedures based on simpler models and more vague information are implemented at the large-scale. Aleatoric uncertainties mainly come out from the modelling of subsoil and structures. The studied example of San Carlo Emilia, that represents a benchmark thanks to the high density of information collected after the May 2012 earthquakes, proves that uncertainty may be reduced adding information and interpreting them with appropriate criteria. Geostatistical analyses of the subsoil investigation are very useful to highlight inconsistent information but, moreover, to quantify uncertainty and eventually plan integrative investigations as estimates are dealt as statistical variables (see Fig.4). Although a detailed knowledge of the structural characteristics of buildings was not possible, the role of construction age is evident, being damage more concentrated on older buildings (Fig. 11).

Epistemic uncertainties on the subsoil mainly concern the simple three layers schematization of the subsoil (a base, a liquefiable layer and a crust). The more complex phenomenology of liquefaction in multilayered soils (see Fig.5) reduces the effectiveness of indicators widely adopted to indicate hazard. Even though subsoil in the present case was everywhere referable to this schematization (Fig.6), other remarkable examples (i.e. Cubrinovski et al. 2014) prove the relevance of this limitation. A crucial issue for the building response is the coupling between shaking and liquefaction. More often buildings that have suffered liquefaction do not exhibit ground shaking damage, but few evidences suggest that structures previously damaged by shaking are more vulnerable to liquefaction. A more complex schematization is necessary to predict coupled effects (e.g. Millen et al., 2019). In the present paper, this issue has been neglected and only the damage induced by liquefaction has been considered. This damage in San Carlo proves to be quite well correlated to the absolute settlements of buildings computed with a formula proposed by Karamitros et al. (2013) that accounts for the seismic input with a cumulative energy parameter, for the stratigraphy and mechanical properties of subsoil and for the main characteristics of the building foundation (size, shape and carried load). The extensive application of this formula to the village of San Carlo proves that the computed variable can be assumed as an indicator of the physical damage (EDP).

ACKNOWLEDGMENTS

The authors wish to acknowledge the contribution by the EU funded project LIQUEFACT "Assessment and mitigation of liquefaction potential across Europe: a holistic approach to protect structures/infrastructures for improved resilience to earthquake-induced liquefaction disasters", project ID 700748 funded under the H2020-DRS-2015.

REFERENCES

Arias, A. 1970. A measure of earthquake intensity. Seismic design for nuclear power plants, R. J. Hansen, ed., MIT Press, Cambridge, Mass.

Baecher GB, Christian JT. Reliability and statistics in geotechnical engineering. Chichester, England: Wiley; 2003.

Bardet JP, Tobita T, Mace N, Hu J. Regional modeling of liquefaction induced ground deformation. Earthq Spectra 2002; 18(1): 19–46.

Bird J., Crowley H., Pinho R., Bommer J., 2005, Assessment of building response to liquefaction induced differential ground deformation, Bulletin of the New Zealand Society for Earthquake Engineering, 38-4, Dec. 2005, 215-234.

Bird J., Bommer J., Crowley H., Pinho R., 2006, Modelling liquefaction-induced building damage in earthquake loss estimation, Soil Dynamics and Earthquake Engineering 26 (2006) 15–30.

Bommer, J.J. and Abrahamson, N.A. (2006). Why do modern probabilistic seismic-hazard analyses often lead to increase hazard estimates? Bulletin of Seismological Society of America 96:6, 1967–1977.

Boulanger, R.W. and Idriss, I.M., 2015. CPT-based liquefaction triggering procedure. *Journal of Geotechnical and Geoenvironmental Engineering*, *142*(2), p.04015065

Boulanger, R.; Ziotopoulou, K. 2012. PM4Sand (Version 2): a sand plasticity model for earthquake engineering applications. *Report no. UCD/CGM-12/01, center for Geotechnical Modeling*.

Campbell, K. W., and Bozorgnia, Y. 2012. A Comparison of Ground Motion Prediction Equations for Arias Intensity and Cumulative Absolute Velocity Developed Using a Consistent Database and Functional Form. Earthquake Spectra, 28(3),931-941.

Cetin, K. O., Seed, R. B., Der Kiureghian, A., Tokimatsu, K., Harder, L. F., Kayen, R. E., and Moss, R.E. S. (2004). Standard penetration test-based probabilistic and deterministic assessment of seismic soilliquefaction potential, J. Geotechnical and Geoenvironmental Eng., ASCE 130(12),1314–1340.

Chilès, J. P. and Delfiner, P. (2012) Geostatistics: Modeling Spatial Uncertainty, 2nd Edition – Wiley - ISBN:978-0-470-18315-1, p. 726.

Comerio, M.C. (editor) (2005). PEER testbed study on a laboratory building: exercising seismic performance assessment. PEER Report. PEER 2005/12.

Cornell, C.A. and Krawinkler, H. (2000). Progress and Challenges in Seismic Performance Assessment. PEER Center News, 3, 1-3.

Cubrinovski M., van Ballegooy S. (2017), System response of liquefiable deposits, 3rd Int. Conf. on Performance Based Design in Earthquake Geotechnical Engineering.

DPC, 2017, Dipartimento della Protezione Civile, Microzonazione sismica, Linee guida per la gestione del territorio in aree interessate da liquefazione (LQ), versione 1.0, Roma (in italian), 57 pp.

Fardis, M.N. et al. (2005). Designers' Guide to EN 1998-1 and EN 1998-5. Eurocode 8: Design of Structures for Earthquake Resistance. General rules, seismic actions, design rules for buildings, foundations and retaining structures. Eurocode Expert, ICE and Thomas Telford, UK.

FEMA/NIBS, 1998. HAZUS - Earthquake Loss Estimation Methodology. Vol. 1, 1998.

Fioravante, V. et al. (2013) Earthquake geotechnical engineering aspects: the 2012 Emilia Romagna earthquake (Italy). *Seventh international Conference on Case Histories in Geotechnical Engineering*, April 29 th – May 4th, 2013. Chicago (US)

Grant R., Christian J.T. and Vanmarcke E.H., 1974, Differential settlement of buildings, Journal of Geotechnical Engineering Division, ASCE, 100(9), pp. 973-991.

Idriss, I.M., Boulanger, R.W., 2010. SPT-based liquefaction triggering procedure. Report # UCD/CGM-10/02 of the Center for Geotechnical Modeling, 259 pp.

Itasca Consulting Group, Inc. (2016) FLAC — Fast Lagrangian Analysis of Continua, Ver. 8.0. Minneapolis: Itasca.

Iwasaki, T.; Tatsuoka, F.; Tokida, K.; Yasuda, S. 1978. A Practical method for assessing soil liquefaction potential based on case studies at various sites in Japan. [conference]: 2nd International conference on Microzonation. - 1978: 885-896.

Karamitros, D.K., Bouckovalas, G. D., Chaloulos Y.K., 2013. Seismic settlements of shallow foundations on liquefiable soil with a clay crust. *Soil Dynamics and Earthquake Engineering*. 46. 64-76.

Karimi, Z. and Dashti, S. (2017) Ground motion intensity measures to evaluate II: the performance of shallow-founded structures on liquefiable ground. Earthquake Spectra, 33(1),277-298.

Krawinkler, H. (editor) (2005). Van Nuys Hotel building testbed report: exercising seismic performance assessment. PEER Report. PEER 2005/11.

Lee, T.-H. and Mosalam, K.M. (2006). Probabilistic seismic evaluation of reinforced concrete structural components and systems. PEER Report. PEER2006/04.

Macaulay T., 2009, Critical Infrastructures, Taylor & Francis, 342 pp.

Madiai C., Vannucchi G., Baglione M., Martelli L., Veronese T. (2016) Utilizzo di prove penetrometriche statiche a punta meccanica per la stima del potenziale di liquefazione, Rivista Italiana di Geotecnica 3/16, pp.14-24.

Millen, M., Ferreira, C., Quintero, J., Gerace, A. and Viana da Fonseca, A. (2019). Simplified equivalent soil profiles based on liquefaction performance. 7th International Conference on Earthquake Geotechnical Engineering. Rome, Italy.

Mitrani-Reiser, J., Haselton, C.B., Goulet C., Porter, K.A., Beck, J., and Deierlein G.G. (2006). Evaluation of the seismic performance of a code-conforming reinforced-concrete frame building - part II: loss estimation. *8th NCEE*, San Francisco, California, April 18-22, 10 pp.

Moehle, J.P. (2003). A framework for performance-based earthquake engineering. *Proc. ATC-15-9 Workshop on the Improvement of Building Structural Design and Construction Practices*, Maui, HI, June.

NZGS, 2016, Earthquake geotechnical engineering practice, Module 2: Geotechnical investigations for earthquake engineering, New Zealand Geotechnical Society and Ministry of Business Innovation & Employment (MBI E) Earthquake Geotechnical Engineering Practice in New Zealand, 44 pp.

NZGS, 2016; New Zealand Geotechnical Society, Earthquake Geotechnical Engineering Practice, Module 3: identification, assessment and mitigation of liquefaction hazards, New Zealand Geotechnical Society and Ministry of Business Innovation & Employment (MBI E) Earthquake Geotechnical Engineering Practice in New Zealand,

Porter, K.A. (2003). An overview of PEER's Performance-based earthquake engineering methodology, *ICASP9*, Civil Engineering Risk and Reliability Association (CERRA), San Francisco, CA, July 6-9.

Poulos, H.G., Carter J.P., Small J.C., 2001, Foundations and retaining structures: research and practice, Proc. XV ICSMGE, Istanbul, vol.4, pp.2527-2606.

Rauch AF, Martin JR. EPOLLS model for predicting average displacements on lateral spreads. ASCE J Geotech Geoenviron Eng 2000;126(4):360–371.

RER, 2012, Primo rapporto sugli effetti della liquefazione osservati a S. Carlo, frazione di S. Agostino (Provincia di Ferrara) - Regione Emilia Romagna Servizio Geologico e dei Suoli e Protezione Civile Ufficio Rischio Sismico e Vulcanico (in italian).

Robertson, P.K. and Wride, C.E. (1998) 'Evaluating Cyclic Liquefaction Potential Using the Cone Penetration Test,' Canadian Geotechnical Journal 35, 442–459.

Tokimatsu K, Seed HB. Evaluation of settlements in sands due to earthquake shaking. ASCE J Geotech Geoenviron Eng 1987;113(8): 861–878.

Toprak, S., Holzer, T. L., Bennett, M. J., Tinsley, J. C. (1999). "CPT- and SPT-based probabilistic assessment of liquefaction potential". Proceedings of Seventh US Japan Workshop on Earthquake Resistant Design of Lifeline Facilities and Counter-measures Against Liquefaction, T. D. O'Rourke, J. P. Bardet, and M. Hamada, eds., Report MCEER-99-0019, MCEER, NY.

van Ballegooy, S.; Malan, P.; Lacrosse, V.; Jacka, M.E.; Cubrinovski, M.; Bray, J.D.; O'Rourke, T.D.; Crawford, S.A.; Cowan, H. 2014. Assessment of Liquefaction-Induced Land Damage for Residential Christchurch. Earthquake Spectra (30) No. 1: pages 31–55, February 2014.

Viggiani, C., Mandolini, A., Russo, G., 2012, Pile and piled foundations, Taylor & Francis, 278 pp.

Yasuda S., Ishikawa K. (2018): Liquefaction-induced Damage to Wooden Houses in Hiroshima and Tokyo during Future Earthquakes. 16 ECEE, Thessaloniki, Greece, June 2018.

Youd TL, Hansen CM, Bartlett SF. Revised multilinear regression equations for prediction of lateral spread displacement. ASCE J Geotech Geoenviron Eng 2002;28(12):1007–1017.

Youd TL, Perkins DM. Mapping of liquefaction severity index. ASCE J Geot. Eng 1987;113(11):1374–1392.

Youd, T. L., and Perkins, D. M. (1978). Mapping Liquefaction-induced Ground Failure Potential, J. Geotech. Eng. Div., ASCE, 104, 433–446pp.

Zhang, G.; Robertson, P.K.; Brachman R.W.I. 2002. Estimating liquefaction-induced ground settlements from CPT for level ground. Canadian Geotechnical Journal 39: 1168–1180.

Zhang, G.; Robertson, P.K., Brachman, R.W.I. 2004. Estimating liquefaction-induced Lateral Displacements from CPT for level ground. Journal of Geotechnical and Geoenvironmental Engineering. AUGUST2004.


Taylor & Francis
Taylor & Francis Group
http://taylorandfrancis.com